Energy Balance in a Radio Frequency Electro-thermal Thruster with Water Propellant

IEPC-2009-203
Presented at the 31st International Electric Propulsion Conference,
University of Michigan • Ann Arbor, Michigan • USA
September 20 – 24, 2009

M. Oya[1], N. Ymamoto[2], and H. Nakashima[3]
Kyushu university, Kasuga, Fukuoka , 816-8580, Japan

Abstract: An energy balance in an inductively coupled radio frequency electrothermal thruster using water as a propellant was investigated with the objective of improving its performance. Absorption efficiency was estimated by means of an *I-V* sensor, and thrust efficiency was estimated by means of a pendulum thrust stand. The absorption efficiency of the thruster using water was 0.75, which is worse than that using argon. Since the number density using water would be less than that using argon due to the low ionization coefficient and power consumption for dissociation. Thrust, specific impulse and thrust efficiency were 3.6 mN, 340 sec, and 0.05, respectively, under the condition water mass flow rate =1.1 mg/s, and incident power = 100 W. Laser absorption spectroscopy system was built in order to estimate the specific enthalpy of the thrusters. The optical system was demonstrated successfully using argon.

Nomenclature

A_{ki}	=	Einstein coefficient
c	=	velocity of light
C	=	capacitance
E_i	=	energy of state i
E_k	=	energy of state k
F	=	thrust
F_1	=	thrust with plasma
F_2	=	thrust without plasma
g	=	acceleration of gravity
g_i	=	statistical weight at absorption state
g_k	=	statistical weight at excited state
I	=	probe laser intensity
I_0	=	incident laser intensity
I_P	=	inductively RF current
I_{sp}	=	specific impulse
j	=	unit imaginary number
k	=	absorption coefficient
K	=	integrated absorption coefficient
k_B	=	Boltzmann constant
M_A	=	atomic mass
$\dot{m}$	=	mass flow
P	=	plasma absorption power

[1] Graduate student, Department of Advanced Energy Engineering Science, hagakure@aees.kyushu-u.ac.jp.
[2] Assistant professor, Department of Advanced Energy Engineering Science, yamamoto@aees.kyushu-u.ac.jp.
[5] Professor, Department of Advanced Energy Engineering Science, nakashima@aees.kyushu-u.ac.jp.

P_i = incident power
R_p = plasma resistance
T = RF period
T_e = electron temperature
v = velocity of atom
V_M = measurement voltage
V_{RF} = RF voltage
x = coordinate in the laser pass direction
Δv_D = Doppler width
λ = wavelength
η_p = absorption efficiency
η_t = thrust efficiency
ν = laser frequency
ν_0 = center absorption frequency
ω = angular frequency

I. Introduction

Electric propulsion systems are desirable propulsion system for a variety of space missions, such as deep space probes, monitoring weather and among other missions, since specific impulse of electric propulsions will be considerably higher than that of chemical rockets.

Recently, several developments have been conducted on small satellites, since they have attractive advantages such as low cost and short development period [1, 2]. Until recently, however, size restrictions have limited the capacity of the available propulsion systems. Hence, the demand for mN class miniature propulsion systems is expected to grow in the future. The adaption of small electric propulsion into small satellites will expand the ability of them and they would be widely used instead of conventional large satellites[3, 4]. A miniature radio frequency electro-thermal (RF) thruster [5-9] is one of the candidates for use as miniature propulsion system. RF thrusters have many advantages in comparison with other propulsions. First, RF thrusters produced high thrust density with relatively high specific impulse (~800 sec). Secondly, plasma of RF thrusters is generated by electrodeless discharge. Thirdly, manufacturing of RF thrusters would be much simpler than other thruster and less complicated installation into a spacecraft. In inductively coupled plasma, RF electrical energy is delivered to the coil wrapped around the quartz tube chamber in order to ionize and heat the propellant gas, thus generating plasma within the discharge chamber. Enthalpy of heated propellant by an ohmic heating of eddy currents converts into axially kinetic energy through a nozzle, then thrusters get thrust from reaction force of kinetic energy. There have been many studies about RF thruster [5-9].

For application of propulsion system to small satellites, size restriction is a hard problem to be overcome. Water is used as a propellant instead of rare gases or hydrogen, since water has alternative characteristics as a propellant, high density, low toxicity, wide availability, and ease of storage and transport. We had been developing a RF thruster using water as a propellant, but the thrust efficiency was 0.003 [10]. It was far from practical application. Hence, the purpose of this study is to investigate the energy balance of the RF thruster in order to improve the thrust performance.

II. Experimental apparatus

A. RF thruster

Experimental apparatus to estimate absorption efficiency is shown in Fig. 1. It was estimated by means of an *I-V* sensor. Thrust measurement experiment was done the same condition as *I-V* sensor measurement but it set inside a chamber. The number of turns of antennas (1mm in a diameter copper wire) and the length were 25 turns and 30 mm, respectively. A quartz tube, (18 mm in the outside diameter and 150 mm in length) was used as a discharge tube. RF electrical energy is delivered to the antenna with 3 MHz in all experiment. Pressure in the discharge tube was measured by means of ceramic capacitance manometric (Ulvac, CCMT-1000A). The pumping system comprised a mechanical booster pump and rotary pump. The background pressure was maintained below 40 Pa for most of the operating conditions.

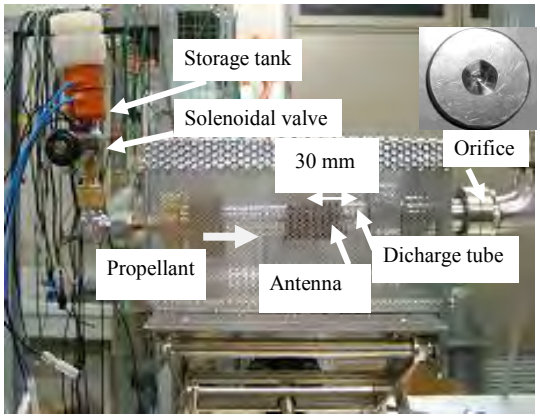

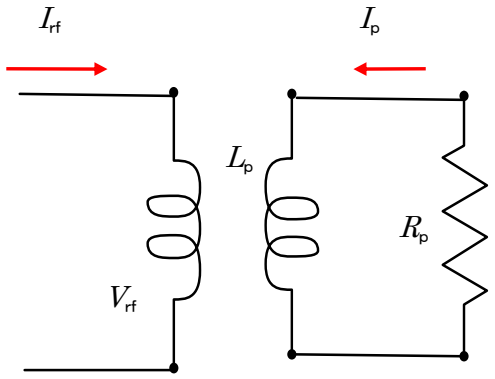

Figure 1. Picture of a plasma measurement system. Figure 2. Equivalent circuit of a RF thruster.

A mass flow was controlled by conductance of needle valve. However, the mass flow control had a problem; mass flow rate suddenly increase due to coexistence of liquid state and gas state. So mass flow was controlled by changing temperature of the propellant tank using a heater surrounded it, since water vapor pressure is proportional to temperature. Mass flow rate was evaluated by measuring mass loss of tank between before and after operation.

B. *I-V* sensor

An equivalent circuit of a RF thruster for the estimation of the absorption efficiency is shown in Fig. 2. The incident current, voltage, and phase angle between them, into the antenna were measured by *I-V* sensor which is set up between RF power supply and antenna. The current is sensed with a pickup loop. The loop captures magnetic flux from the current carrying conductor, which creates a voltage in the loop (recall Faraday's Law and Biot-Savart Law). The V_M depends on coupling capacitance and electronics impedance. The relation between RF voltage and electric potential is expressed as

$$V_M = V_{RF} \frac{50}{\frac{-j}{\omega C} + 50} \tag{1}$$

Each of the voltage and current were read out by digital oscilloscope.

C. Thrust stand

The thrust efficiency was estimated by a thrust stand. The pendulum type thrust stand was used for the thrust measurement as shown in Fig. 3. The displacement of the pendulum was measured by a load cell (Kyowa industry

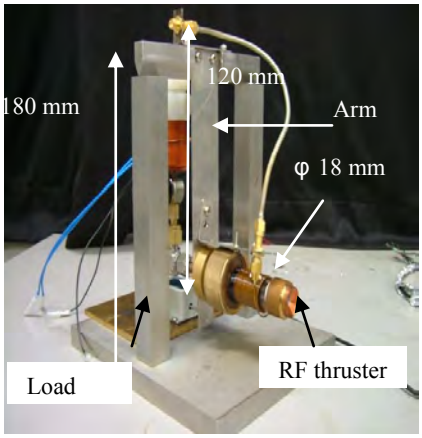

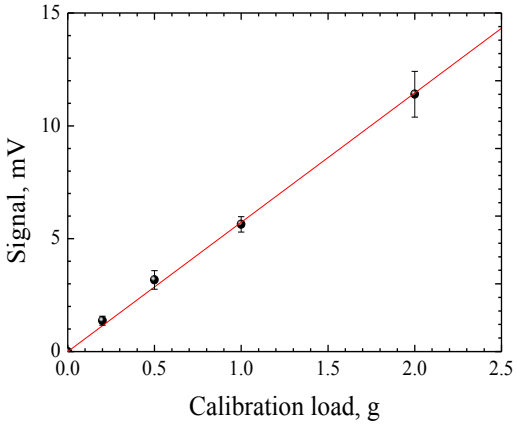

Figure 3. Thrust stand for thrust measurement. **Figure 4. Calibration results of the thrust stand developed**

products, LTS-50GA). This thrust stand was designed for use the experiment in a 267 mm diameter and 400 mm long vacuum chamber. Relation between calibration load and signal is shown in Fig. 4. The characteristic frequency of this pendulum type thrust stand was 1.4 Hz, it would be thought that there is no effect factor of resonance from any oscillating source. Calibration of the thrust stand was operated changing a weight from 0 g, to 0.2 g, 0.5 g, 1.0 g and 2.0 g. The error of this measuring apparatus would be caused as below. At first, the standard deviation of 0 g, 0.2 g, 0.5 g, 1.0 g and 2.0 g were 0.20 mV、0.41 mV、0.33 mV and 1.0 mV respectively. The error of each standard deviate were 15 %、13 %、6.0 % and 8.8 % respectively. The error from S/N ratio which was 370 was calculated 0.27 %. This could be neglected. Furthermore, the error of fitting was R^2=0.998, so the errors were estimated 14 % and 6 % at the thrust were 2.0 mN, 10 mN respectively

III. Result and discuss

Absorption efficiency [11] and thrust efficiency are defined as follows.

$$P_{\mathrm{p}} = \frac{\int_0^T \frac{1}{2} I_{\mathrm{p}}{}^2 R_{\mathrm{p}} dt}{T} \tag{1}$$

$$\eta_{\mathrm{p}} = \frac{P_{\mathrm{p}}}{P_{\mathrm{i}}} \tag{2}$$

$$I_{\mathrm{sp}} = \frac{F}{\dot{m} g} \tag{3}$$

$$\eta_{\mathrm{p}} = \frac{F_1{}^2 - F_2{}^2}{2\dot{m} P_{\mathrm{i}}} \tag{4}$$

A. Absorption efficiency

The input power was measured by means of a power-meter. A plasma absorption power was estimated from the current and the voltage trace, which were measured by means of an *I-V* sensor.

Absorption efficiency for different gas is shown in Fig. 5. Absorption efficiency using water for P_{i} = 100 W and 200 W were 0.75, 0.8, respectively. That is, the absorption efficiency increased with increase in incident power. This improvement would be due to the transformation from capacitive coupling to inductive coupling, which results from increase in plasma density in the discharge tube. As shown in Fig. 6, emission from the plasma was seen at upstream side from the antenna under the condition of low incident power. However, with increase in incident power, strong emission region moved to the vicinity of the antenna. In addition, with increase in incident power, emission intensity of plasma became strong. These results supported above assumption.

The absorption efficiency using argon was higher than that using water. For P_{i} = 100 W, the absorption efficiency using water, and that using argon were 0.75 and 0.91, respectively. This is due to the increase in loss of circuit since the circuit current using water was 1.8 times larger than that of using argon. The number density using water would be less than that using argon due to the low ionization coefficient and power consumption for dissociation. Thus, the absorption efficiency using water was worse than that using argon, although specific enthalpy of water was larger than that of argon, which were 91 MJ/kg and 11 MJ/kg, respectively.

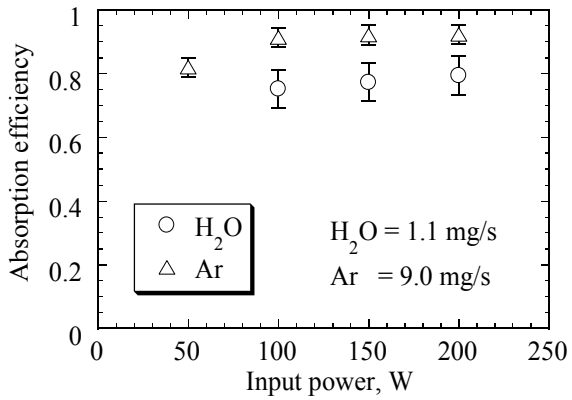

Figure 5. Absorption efficiency for different gases.

B. **Thrust measurement**

Relation between mass flow rate and thrust using water, at P_i = 100 W, is shown in Fig. 7. For $\dot{m}$ = 1.1 mg/s, thrust without plasma was 1.4 mN, and the thrust with plasma was 3.6 mN. The thrust at $\dot{m}$ = 1.1 mg/s, 1.9 mg/s, and 2.5 mg/s are 3.6 mN, 6.1 mN, and 6.1 mN, respectively. That is, the thrust was increased with increase in mass flow rate. The relation between specific impulse and thrust efficiency is shown in Fig.8. The specific impulse and the thrust efficiency was 340 s at $\dot{m}$ = 1.1 mg/s. With increase in mass flow rate, the specific impulse decreased. This might be due to decrease in temperature of high enthalpy flow due to the decrease in specific enthalpy. The thrust efficiency was 0.05 at $\dot{m}$ = 1.1 mg/s. The thrust efficiency is improved in comparison with our previous study [10]. This would be due to the decrease in heat loss at wall surface since a diameter of a quartz tube is 10 mm in our previous study; a diameter of the present quartz tube is 1.8 times larger than that one. From the result of thrust efficiency, there was an optimum mass flow rate. This tendency is due to the tradeoff between coupling of plasma and specific enthalpy. With increase in mass flow rate, the plasma coupling was improved, which resulted from the increase in plasma density, however, specific enthalpy decreased.

Energy balance in RF thruster using water is shown in Fig. 9. Only 5 W was converted to kinetic energy from incident RF power. In order to improve the performance of RF thruster, heat loss needs to be recovered by regenerative cooling.

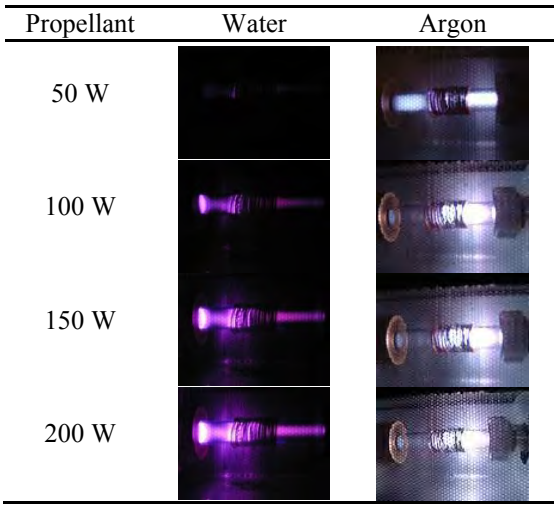

Figure 6. Picture of RF plasma for different power.

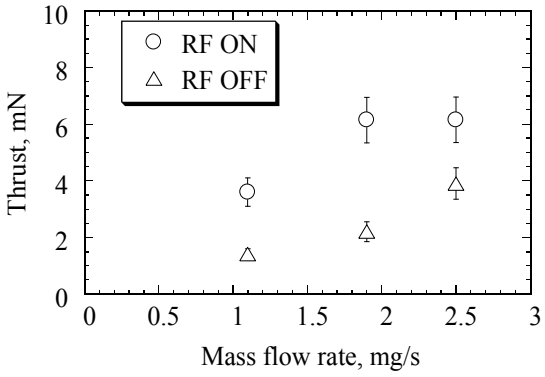

Figure 7. Relation between mass flow rate and thrust.

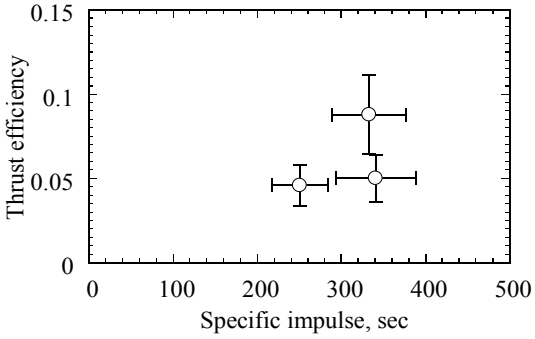

Figure 8. Relation between Specific impulse and thrust efficiency.

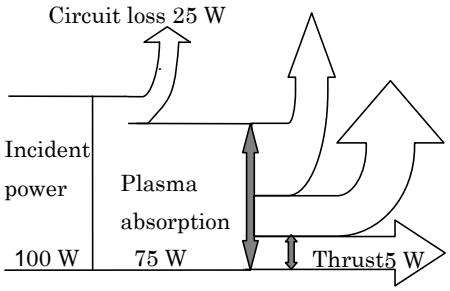

Figure 9. Energy balance in RF thruster using water.

IV. Laser absorption spectroscopy (LAS) system

A. Temperature measurement

As shown in Fig.9, the rest of energy was estimated as heat loss, frozen flow loss and nozzle loss. Laser absorption spectroscopy (LAS) was chosen as a diagnostics for measuring specific enthalpy of our thrusters, in order to investigate the detail of the rest energy. The absorption profile of atomic lines has information such as its wavelength, intensity and shape[12]. From such information, translational temperature and flow velocity of the absorbing atom can be deduced. These parameter can be obtained by LAS. From specific enthalpy, enthalpy transfer efficiency which indicates how much the power translated from plasma to propellant species is estimated. The thrust can be estimated by flow velocity which is estimated using the Doppler shift of a spectral line. The frozen flow loss can be estimated by species density which is estimated using integrated absorption coefficient.

The relationship between incident laser intensity I_0, probe laser intensity I and absorption coefficient $k(\nu)$ is expressed by the Beer-Lambert law as [13]

$$\int k(\nu)\mathrm{d}x = -\ln\left(\frac{I}{I_0}\right) \tag{5}$$

Absorption profile is broadened by various physical mechanisms, and is expressed by a convolution of the Lorentz and the Gauss distribution [14]. Since, in our experimental conditions, Doppler broadening is dominant and other broadenings such as natural, pressure and Stark one are all neglected, the absorption profile $k(\nu)$ at the frequency ν is approximated to be Gauss distribution expressed as [15],

$$k(\nu) = \frac{2K}{\Delta\nu_D}\sqrt{\frac{\ln 2}{\pi}}\exp\left[-\ln 2\left\{\frac{2(\nu-\nu_0)}{\Delta\nu_D}\right\}^2\right] \tag{6}$$

Here, ν_0 is the center absorption frequency and K is the integrated absorption coefficient. Doppler broadening $\Delta\nu_D$ is the statistical one originating from thermal motion of the particle and related to the translational temperature expressed as [16],

$$\Delta\nu_D = \frac{\sqrt{8R\ln 2}}{\lambda}\sqrt{\frac{T_t}{M_A}} \tag{7}$$

In this study, the target of an absorption line was 826.456 nm from meta-stable state. The transition data for this measurement are shown in Table 1, as quoted from the NIST database [17].

Table 1. Transition data for argon (from NIST database)

λ, nm (Air)	826.45
E_i, eV	11.828
E_k, eV	13.327
A_{ki}, S^{-1}	1.53×10^7
g_i	3
g_k	3

B. Optical system

The schematic of optical system and the picture of optical apparatus are shown in Fig. 10. A single longitudinal mode diode-laser (HL8325G, HITACHI Ltd., LDC205C, Thorlabs Inc.) was used as the laser oscillator. The laser frequency monitored by a spectrometer was roughly matched to the absorption one by temperature control (TED200C; Thorlabs Inc.). Then, it was scanned over the absorption line shape by current modulation with a function generator. The optical isolator was used to prevent the reflected laser beam from returning into the diode-laser. The beam was divided into four beams by beam splitters. The first beam going through a plasma of the reference cell was detected by photo detector (PD). The second beam goes through solid etalon, finesse of 30, free spectral range (FSR) was 1.146 GHz at 826.45 nm. The third is used as a-wavelength monitor by spectrometer. The fourth goes through the RF plasma and detected by PD. To eliminate the influence of plasma emission, a band pass filter at 820nm, whose full width half maximum (FWHM) is 10 nm was used. All signal ware recorded using a PC based data acquisition system (WE7000; Yokogawa Co.).

C. Absorption profiles

The normalized absorption profile and Gauss fit are shown in Fig. 11. A FWHM of absorption profile was obtained by Gauss fitting, and transitional temperature can be estimated from the FWHM. Relation between incident RF power and transitional temperature is shown in Fig. 12. The transitional temperature for P_i = 50 W, 100 W, 150 W, 200W and 250 W, were 529 K, 607 K, 644 K, 844 K and 1065 K, respectively at mass flow rate = 0.3 mg/s ; That is, with increase in incident power, the transitional temperature was increased owing to the increase in specific enthalpy. Relation between mass flow rate and transitional temperature, at P_i = 250 W, is shown in Fig. 13. The transitional temperature was increased with increase in mass flow rate. This would be because the RF energy was converted efficiently to heavy particle due to increase in collisions.

In this experiment, LAS system was built in order to estimate for the specific enthalpy of the thrusters. The optical system was demonstrated successfully.

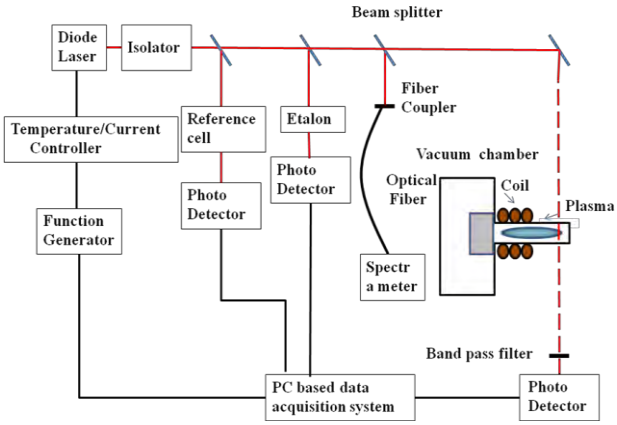

Figure 10. Schematic of optical system

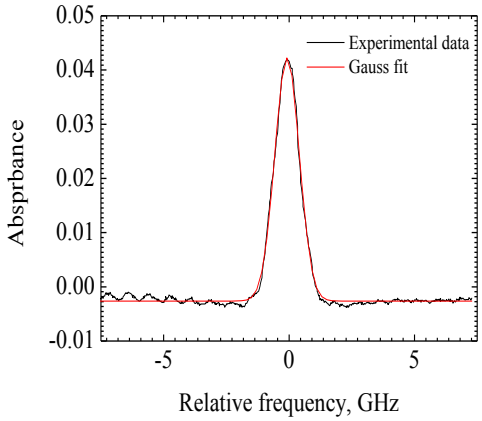

Figure 11. Absorption profile and Gauss fitting

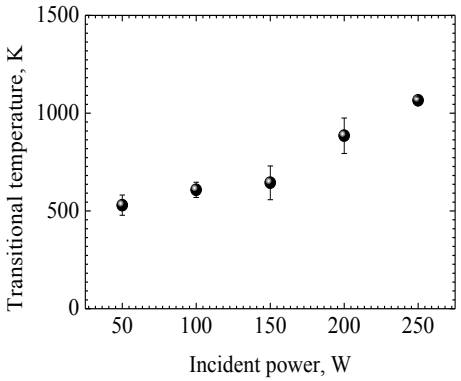

Figure 12. Relation between incident power and Transitional temperature.

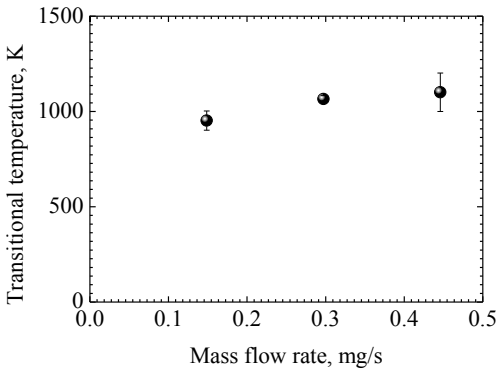

Figure 13. Relation between mass flow rate and Transitional temperature.

V. Conclusion

An energy balance in an RF thruster using water as a propellant was investigated with the objective of improving the thrust performance. The results obtained are as follows.

1. Absorption efficiency was estimated by means of an *I-V* sensor. Absorption efficiency using water for P_i = 100 W and 200 W were 0.75, 0.8, respectively. The transformation from capacitive coupling mode to inductively coupling mode, which results from increase in plasma density, led to the improvement of the absorption efficiency. The absorption efficiency using argon was higher than that using water. This is due to the increase in loss of circuit; the circuit current using water was 1.8 times larger than that of using argon. The number density using water would be less than that using argon due to the low ionization coefficient and power consumption for dissociation.
2. The thrust performance, thrust, specific impulse and thrust efficiency were 3.6 mN, 340 sec, and 0.05, respectively, at $\dot{m}$ = 1.1 mg/s, and P_i = 100 W. There was an optimum mass flow rate for the thrust efficiency. This tendency is due to the tradeoff between coupling of plasma and specific enthalpy.
3. Laser absorption spectroscopy (LAS) was built in order to estimate for the specific enthalpy of the thruster. The optical system was demonstrated successfully. A transitional temperature was 576 K at incident power = 100 W, mass flow rate = 0.15 mg/s.

In future work, the specific enthalpy is estimated by means of LAS, in order to investigate for heat loss of the RF thruster. The LAS system is applied to the RF thruster using water propellant. The target of an absorption line is 656.28 nm from H atoms.

References

[1]Kato, M., Takayama, S., Nakamura, U., Yoshihara, K. and Hashimoto, H.: Road Map of Small Satellite in JAXA, 56th International Astronautics Congress, 2005, pp. IAC-05.B5.6.B.01.

[2]Sahara, H., Nakasuka, S. and Kobayashi, C.: Propulsion System for Panel ExTension SATellite (PETSAT), *AIAA* Proceedings of 41st Joint Propulsion Conference and Exhibit, Tucson, Arizona, USA, July 10-13, (2005). pp. 2005-3956.

[3]Mueller, J.: Thruster Options for Microspacecraft: A Review and Evaluation of State-of-the Art and Emerging Technologies, Progress in Astronautics and Aeronautics, Vol.187, *AIAA*, Reston, 2000, pp. 45–137

[4]Mueller, J., Marrese, C., Polk, J., Yang, E., Green, A., White, V., Bame, D., Chadraborty, I. and Vargo, S.: An Overview of MEMS-Based Micropropulsion Development at JPL, *Acta Astronautica*, Vol. 52, Nos. 9-12, 2003, pp. 881-895.

[5]Pollard, J., E.Lichtin, D. and A.Cohen, R. B**.**: RF Discharge Electrothermal Propulsion: Results from a Lab-Scale Thruster, *AIAA J.*, **23** (1987), pp. 1987-2124.

[6]Thomas. S. R., Micheal. M. M. and Sven. G. B.:Design and Initial Tests of a Low Power Radio-Frequency Electrothermal Thruster, *AIAA J.,*(2008), pp.2008-4537

[7]Brewer, L., Frind, G., Karras, T. and Holmes, D.G.: Preliminary Results of a High Power RF Thruster Test, *AIAA*, (1989), pp. 89-2382

[8]Olson, L.: Operation of a 50 watt RF Plasma Thruster, *AIAA J, (*2001) pp. 2001-3903.

[9]Mironer, A. and Hushfar, F.: Radio frequency heating of a dense moving plasma *AIAA*, (1963) pp.1963-45.

[10]Ogawa, S.: Master thesis, Kyushu University, Fukuoka, 2005. (in Japanese)

[11]Lieberman, M. A. and Lichetenberg, A. J.: Principles of plasma discharges and materials processing, ED research Co. pp. 285-303

[12]Matsui, M. Satoshi, O., Komurasaki, K. and Arakawa, Y.: Influence of Laser Intensity on Absorption Line Broadening in Laser Absorption Spectroscopy, Journal of Applied Physics, Vol. 100 (2006), pp. 063102

[13]Baer,D.S., Nagali,V., Furlong,E.R,K, and New-field, M.E.: Scanned - and Fixed – Wavelength Absorption Diagnostics for Combustion Measurements Using Multipulexed Diode Laser, *AIAA J.,***34** (1996), pp. 489-493.

[14]Matsui, M., Ikemoto, T., Takayanagi, H., Komurasaki, K. and Arakawa, Y.: Generation of Highly Dissociated Oxygen Flows by a Constrictor-type Arc-heater, Vol. 21, No.1 (2007), pp247-249.

[15]Hanson,R. K..: Absorption Spectroscopy in Scooting Flames Using a Tunabke Diode Laser, Appl. Opt., **19** (1980), pp.482-484

[16]Matsui, M., Komurasaki, K., Gerorg H. and Monika, A-K.: Inductively Heated Plasma Generator Flow by Laser Absorption Spectroscopy, AIAA Journal、Vol. 43, No. 9 (2005) pp.2060-2064.

[17]http://physics.nist.gov/PhysRefData/ASD/lines_form.html